# A New Propelled Wing Aircraft Configuration

**Conference Paper** · November 2016

DOI: 10.1115/IMECE2016-65373



**3 authors:**

-Michele Trancossi-
Sheffield Hallam University
**148** PUBLICATIONS **730** CITATIONS
SEE PROFILE

Jill Stewart
University of Derby
**32** PUBLICATIONS **138** CITATIONS
SEE PROFILE

José Páscoa
Universidade da Beira Interior
**172** PUBLICATIONS **718** CITATIONS
SEE PROFILE

**Proceedings of the International Mechanical Engineering Congress and Exposition 2016**
**IMECE16**
**November 11 – 17, 2016, Phoenix, AZ, USA**

# IMECE2016-65373

# A NEW PROPELLED WING AIRCRAFT CONFIGURATION

**Michele Trancossi**
Sheffield Hallam University
Sheffield, South Yorkshire, UK
m.trancossi@shu.ac.uk

**Jill Stewart**
Sheffield Hallam University
Sheffield, South Yorkshire, UK
j.stewart@shu.ac.uk

**Jose C. Pascoa**
Universitade da Beira Interior
Covilla, Beira, Portugal
pascoa@ubi.pt

## ABSTRACT

This paper investigates by an energetic approach possible new configurations of aircrafts, which can rival in low speed operations against helicopters. It starts from an effective energy balance of helicopters during fundamental operations: takeoff, horizontal flight, hovering, and landing. The energy state of a helicopter can be written as:

$E = ½\, mV^2 + mgh + ½\, I\, \omega^2$ (1)

where m is mass of helicopter, I is total rotor inertia, ω is rotor rotational speed. By taking the partial derivative with respect to time of equation 1, the power is expressed as

$dE/dt = \Delta P = mV\, dV/dt + mg\, dh/dt$ (2)

By optimizing the energy balance of the helicopter a new aircraft configuration has been obtained that allow a very high lift even at very low speed, but drastically reducing the energy consumption during horizontal flight. The total power required is obtained by rotor power and overall efficiency factor (η) and $HP_{req\ total} = \eta\, HP_{req\ rotor}$

By equations (1) and (2) it has been produced a preliminary optimization in different operative conditions considering a speed range from *0.5* (hovering conditions) to *50 m/s*. By an accurate balance of the results, it has been identified that the most disadvantageous situation for a helicopter is forward flight. A new powered wing architecture has been specifically studied for replicating the behaviour of helicopters. Preliminary it has been defined by starting from the energy equations the main characteristics of the propelled wing. From those numerical results it has been defined a new configuration of propelled wing and the new aircraft configuration which allow adequate performance against helicopter. Those wings take a large advantage of two not common features: symmetry with respect to a vertical axis and possibility of optimizing the shape for specific missions.

It has been designed and optimized in different configurations by CFD. In particular, an accurate analysis of fluiddynamic of the system allows quantifying the different effects that allows realizing an extraordinary ratio between lift and thrust producing an effective vehicle that can rival against helicopter also at very low speeds with a morphing configuration that will be presented in the final paper because of patenting reasons. Results show that the proposed innovative aircraft configuration allows hovering and very low speed flight. In particular, the conditions and the design for this kind of operation are presented even if still in initial design stage. The presented aircraft architecture can also allow inverting the direction of motion just by inverting the direction of the thrust. In this case, it will allow overcoming completely the performances of helicopters. The energetic balance of flight has been evaluated and the advantages with respect to helicopters have been finally expressed with surprising results.

## NOMENCLATURE

**Dimensionless coefficients**

| | |
|---|---|
| $C_D$ | Drag Coefficient (-) |
| $C_L$ | Lift Coefficient (-) |
| $\Delta M$ | amount by which advancing blade tip Mach number exceeds drag divergent Mach number, |
| $t_c$ | thrust coefficient, |
| $t_{cdiv}$ | thrust coefficient at which stall power occurs |

**Physical magnitudes**

| | |
|---|---|
| $\delta$ | Distance between vertical thrust and centre of gravity (m) |
| $\varepsilon$ | distance between the point of application aerodynamic lift and centre of gravity (m) |
| $\phi$ | Pitch angle (rad) |
| $\kappa$ | constant coefficient of thrust |
| $\mu$ | advance radius |
| $\Omega$ | Angular velocity of helicopter propeller (rad/s) |
| $\rho$ | Density (kg/m$^3$) |

| | |
|---|---|
| $A$ | Area ($m^2$) |
| $D$ | Drag force (N) |
| $E$ | Energy (J) |
| $Ex$ | Exergy (J) |
| $I$ | Moment of Inertia (kg $m^2$) |
| $I_p$ | moment of inertia of main propeller (kg $m^2$) |
| $I_r$ | moment of inertia of rear rotor (kg $m^2$) |
| $L$ | Lift Force (N) |
| $P$ | Power (W) |
| $R$ | Rotor Radius (m) |
| $T$ | Thrust (N) |
| $V$ | Air speed (m/s) |
| $a$ | Acceleration ($m/s^2$) |
| $b$ | Number of blades (-) |
| c | blade chord (m) |
| $f$ | equivalent flat-plate drag area ($m^2$) |
| $g$ | Gravity (9.81 m/s) |
| $h$ | Height (m) |
| $m$ | mass (kg). |
| $t$ | Time (s) |
| $v$ | Velocity (m/s) |
| $v_i$ | induced velocity (m/s) |
| *EMIPS* | Exergetic Material Input per Unit of Service (J) |

## Pedices

| | |
|---|---|
| D | drag (related to energy and power) |
| K | kinetic (related to energy and power) |
| R | rotor (related to energy and power) |
| T | Thrust (related to energy and power) |
| req | required |
| rot | rotor |
| x | horizontal |
| y | vertical |

## INTRODUCTION

With the development of aviation technology, helicopter has coupled effective performances and flexibility [1-3] with lower energy efficiency than any other vehicle [4].

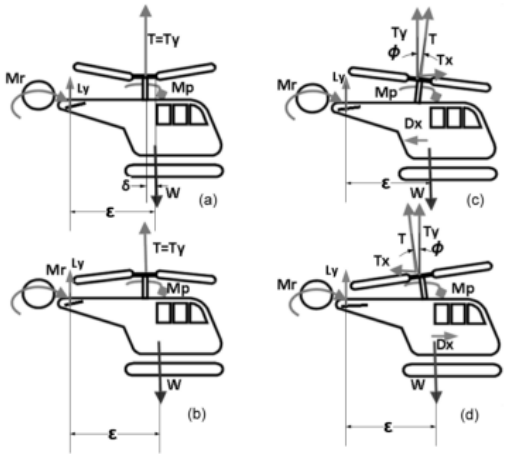


**Figure 1. Forces on a helicopter in different flight conditions.**

This paper takes the moves from the optimization of the energy balance of a helicopter in flight and by optimizing this model arrives to the definition of a new vehicle concept, which can do anything that a helicopter can do with mayor energetic benefits. The forces applied on a helicopter changes in different flight conditions [5] and they are presented in Figure 1.

Possible competitors are tilt rotor aircrafts, such as Boeing Osprey, which allow to couple some of the features of helicopter and some of the features of aircraft. Other potential competitors are still very young in terms of Technology Readiness Level. They are cyclorotors and propulsive wings.

## Energy balance

It is possible to produce an effective definition of a realistic even if simplified energy model that allow weighting the energy needs for different operations, which are necessary for power dimensioning of different flight conditions. According to Wood [1] and Zuang [6] the energy model of a helicopter during flight is given by equation (1):

$$E = \frac{1}{2}mV^2 + mgh + \frac{1}{2}I\Omega^2 \qquad (2)$$

where I is total rotor inertia and Ω is rotational speed.

Dewulf and Van Langenhove [7] has defined EMIPS (acronym of Exergetic Material Input per Unit of Service) analysis, They evaluate transport modes, and vehicles in terms of exergetic material input pro unit of service (EMIPS):

$$R/S = \frac{Ex_{resources}}{Ex_{service}} = \text{EMIPS} \qquad (3)$$

This method allows producing an effective assessment of the sustainability of transport modes in terms of resource productivity, based on the concept of material input per unit of service (MIPS). The amount of resources extracted from the ecosystem to provide the transport service has quantified defining an inventory of all exergetic resources in the whole life cycle. The method allows evaluating cumulative exergy consumption also introducing an effective differentiation between non-renewable and renewable resource inputs according to Gong and Wall [8]. Trancossi [9-10] has modified the model by introducing an effective distinction of the energy needs for moving the vehicle and moving the payload. He does not consider the vehicle as a necessity, but he seeks by this approach to identify how the vehicle can be improved minimize its energy consumption.

## Tilt rotors

Tiltrotors are aircrafts, which can tilt their propellers allowing them to operate with vertical (helicopter mode) or horizontal axis (airplane mode). Current tilt rotors are used in military field, even if some civil vehicles are going to be delivered on the market. They present large problems of instability at low speed and other operative limits [11]. The cross-link drive shaft often presents excessive vibration while wing flexing often damaged the shaft and high disc loading can generate excessive downwash.

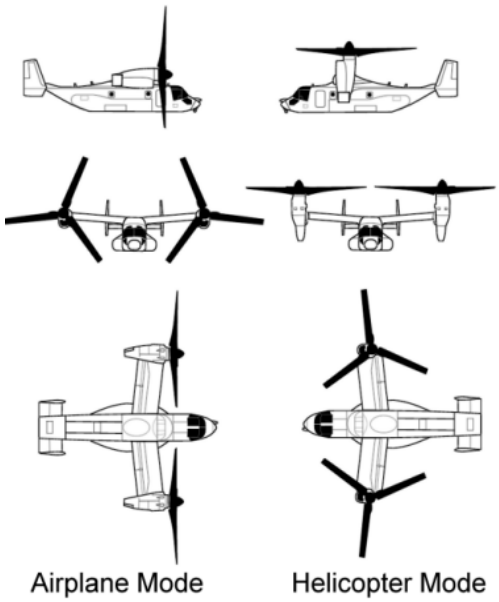


**Figure 2. Tiltrotor aircraft configurations during flight**

Many tilt rotors presents instability problems when wing angle is between 35° and 80°. In the case of V-22 Osprey, another problem is related to very high disc loading. This has contributed to V-22 maintenance problems since vertical landings at unimproved sites produce massive dust clouds that are ingested into its engines [12]. This is why V-22s rarely stray from hard surface runways, and prefer rolling take-offs to outrun any dust. This problem forced to introduce precise limits in operations.

## Cyclorotors

Cyclorotors present large advantages expecially for ground effect vehicles. They resemble the Voith-Schneider propeller [13, 14] for marine use in the aeronautic field (Fig. 1). Cyclorotor is a mobile wing system constituted by rectangular planform shaped wings, which are disposed on a cylinder and rotate around the axis of the cylinder. Wings can perform controlled oscillations around along an axis that intersects the mean chamber line and is parallel to the blade span (Fig. 2). The pitching schedule of the blades is controlled by a mechanical system that should be able to change the direction and magnitude of the rotor resultant thrust vector. This technical solution allows a substantial increase in the aircraft control (Fig.3) [15, 16]. It produces several advantages in comparison with any VTOL rotary or fixed wing air vehicle. It uses common wing surfaces to achieve lift and thrust along the full range of flight speeds. It could reduce the drag by wings at high advance speed. It creates lift, and thrust, when the blades move backward in relation to the vehicle's direction of flight.

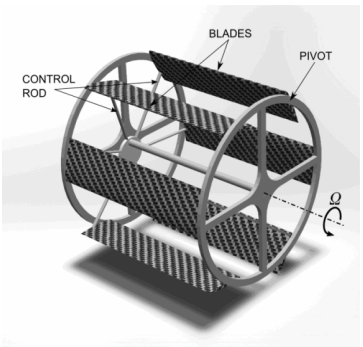


**Figure 3. 3D representation of a cyclorotor with six NACA0012 blades and a max pitch angle of 40 degree.**

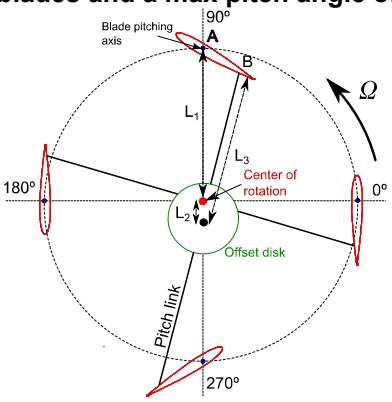


**Figure 4. Configuration for the pitch control mechanism [6].**

In addition, it allows using the intermittent, but very high, lift value generated by the unsteady pitching of the blades. Further, each blade of the cyclorotor operates at similar conditions (angle of attack, velocity, Reynolds number) so the blades can be easily optimized in terms of aerodynamic performance.

The pitching schedule of the blades generates an unsteady flow. It could play a significant role in the aerodynamic efficiency of cyclorotors propulsion. It can delay blade stall, thus increasing the amount of lift that can be produced by each blade. Moreover, the rotational speed and pitching schedule of the cyclorotor does not need to increase with vehicle speed, since the achievable thrust increases with forward airspeed for a constant rotor angular velocity.

The possibilities disclosed by cyclorotors seem allowing novel VTOL aircraft architectures. If the design attention is focused on performance, it allows definition of novel air vehicle concepts, which can reach high subsonic speeds and higher energy efficiency than helicopters [17]. Despite their recent improvements, cyclorotors present actual limits in term of affordability at high rotation speed and of induced vibration, which is due to both aerodynamic forces and change in inertia moment.

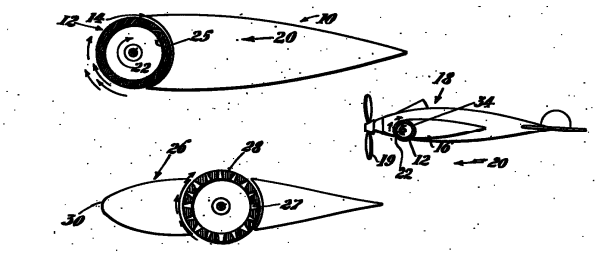

**Figure 5. Magnus effect enhancer or propulsion (1941)**

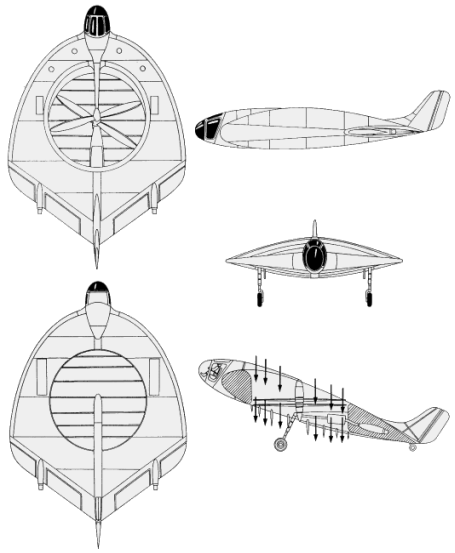

**Figure 6. Forke Wulf VTOL Project (1944)**

## Propelled wings

Another competitor of helicopter is propelled wing architecture. Propelled wings have been designed with multiple concepts that can couple also with diffused propulsion concepts.

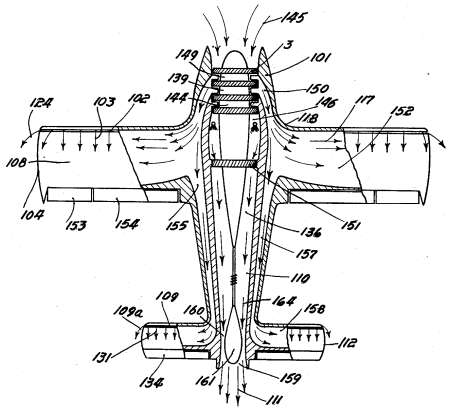

**Figure 7. Henri Coanda multistage propulsion and jet wing discharge concept**

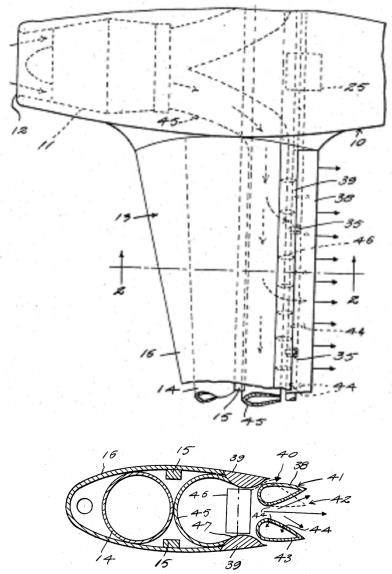

**Figure 8. Jet wing discharge propulsion system (1949)**

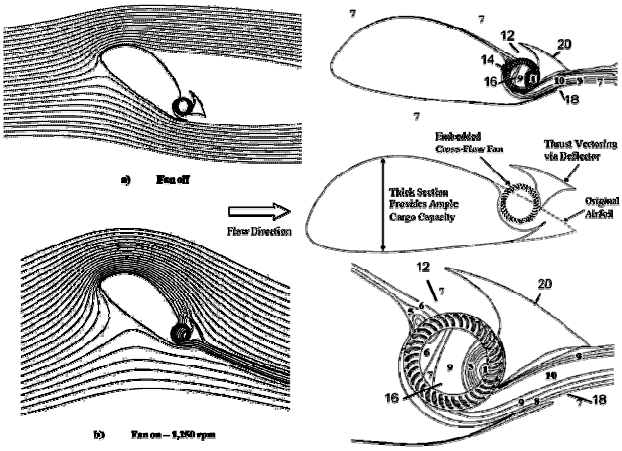

**Figure 9. Propulsive wing system (2006)**

An interesting concept seems to be Magnus Effect enhancer [18], which introduces the possibility of inserting a pass through propeller into a wing (Figure 5). Another important idea seems the Wulf VTOL Project [19] that introduces helicopter propulsion by a turbofan engine and couples counter-rotating helicopter propulsion with an effective mobile deflector system and jet propulsion into the architecture of a flying wing aircraft (Figure 6).

Some concepts couple jet propulsion with wings. One is the concept of jet wing discharge [20, 21] that distributes the jet exhausts by channels inside the wings and coupled with mobile flaps that allows orienting the jet (Figure 7 and 8). Wing-mounted jet-propulsion system with controllable discharge outlet [22] develops a similar concept, by introducing multiple jets inside a wing.

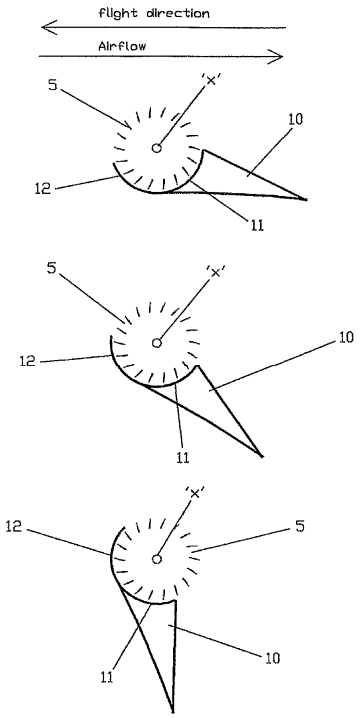


**Figure 10. FanWing arrangements (2006)**

More recently the concepts based on pass-through fans are acquiring an increased interest, because they are capable of generating a significant over lift. For example, The Propulsive Wing [23] has been initially developed at Syracuse University. It replaces the aircraft fuselage conventional fuselage with an extremely thick wing with partially embedded, distributed cross-flow fans for both thrust and flow control. This configuration maintains smooth airflow, increasing lift, decreasing drag, and preventing stall. It also ensures an extremely short ground roll. The cross-flow fan propulsive wing is essentially a modular technology, which can be integrated into a wide array of aircraft, in both size and mission specifications. It seems scalable and easily reconfigurable to meet changing requirements. Cross-flow fans, partially embedded within the airfoil section, draw the flow in from the suction surface and exhaust the flow out at the trailing edge. The fans can be powered by any motor or engine.

The propulsive airfoil has the ability to draw in substantial amounts of air and maintain attached flow regardless of angle of attack, allowing operation at angles of attack over 45 degrees and lift coefficients of more than 10 at take-off and landing. The other competitor is Fanwing [24], which couples cross flow fan with a simpler wing design with respect to Propulsive Wing but with a similar propulsion concept. It allows to flight at very low speed and very high angle of attach.

Crossflow fan architectures present innovative performances in terms of shortening take off and landing spaces but does not allow to perform VTOL operations and hovering. Another system, which allow an effective STOL operations and allows and effective increase of the performance on different aircraft architectures is the more recent ACHEON (Aerial Coanda High Efficiency Orienting-Jet Nozzle) system [24] (Figure 12).

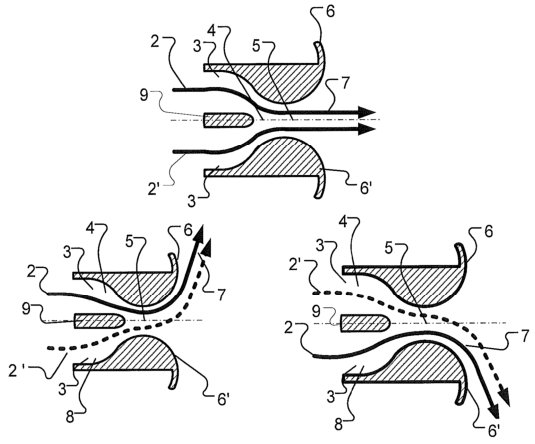


**Figure 11. ACHEON Nozzle**

ACHEON project [25, 26] has demonstrated the possibility of deviating a propulsive synthetic jet, which is generated by two impinging streams, by mean of Coanda effect [27-30]. In particular, it has verified that the deflection angle of the jet (and of the thrust) is a function of both momentums (and speeds) of the two primitive streams and the geometric configuration of the nozzle. The core of the ACHEON thrust and vector propulsion is a nozzle with a duct eventually bipartite into two internal channels, which converge in a single outlet with two facing Coanda surfaces (3) and (3'). Two impinging jets (2) and (2') generate a synthetic jet that proceeds straight if the streams have equal momentums, or adheres to the Coanda surface on the side of the stream with higher momentum. The direction of the synthetic jet depends on the momentums of the two jets. Control and stability are increased by Dielectric Barrier Discharge (DBD) installation [31]. The architecture fits with electric propulsion and subsonic aircrafts (Mach 0÷0.5).

ACHEON produced a large impact on the activity about modelling Coanda Effect [32-34], about modelling Coanda effect in presence of multiple streams [35-43], the potential of Dielectric Barrier Discharge [41-43], and application of the nozzle in aircraft propulsion, including existing aircraft architectures [44-47]. ACHEON has demonstrated very good characteristic in terms both of reduction of energy needs and take off and landing spaces equivalent to the one that can be reached by propelled wing systems.

## ENERGY MODEL OF AN HELICOPTER

The main advantage of helicopter with respect to any other possible competitor is the operative flexibility and general robustness. None of the analyzed alternative solutions to helicopters can emulate helicopters and their flexibility. The one that can replicate better the behaviour of helicopter during operation is certainly the cyclorotor configuration. The

propelled wing based architectures presents different behaviours and different laws of motion and they cannot reply some helicopters manoeuvres such as hovering and reverse flight. Considering the equilibrium of a helicopter moving on a vertical plane, it is possible to express a simplified expression of the equilibrium of the helicopters in a general case:

$$\begin{cases} Ma_x = \Sigma_i Fx \\ Ma_y = \Sigma_i F_y \\ I\dot{\omega}_z = \Sigma_i M_z \\ 0 = \Sigma_i M_y \end{cases} \Rightarrow \begin{cases} Ma_x = T\sin\phi - D_x \\ Ma_y = T\cos\phi + L_y - W - D_y \\ I\dot{\omega}_z = \delta \cdot T \cdot \cos\phi + \varepsilon \cdot L_y \\ M_p + M_r = 0 \end{cases} \quad (4)$$

Those equations allow studying the flight motion of a helicopter on a 2D vertical plane. According to Figure 1, it is possible to describe different flight conditions (Appendix 1). Wood [1] and Zuang [47] have developed helicopters energetic flight models of a helicopter. A measure of the energy state of a helicopter at any altitude airspeed-RPM combination can be expressed as:

$$E = \frac{1}{2}mV^2 + mgh + \frac{1}{2}I_r\Omega^2 \quad (5)$$

The last term of the above equation is the kinetic energy of the rotor. Since most helicopters normally operate at almost constant RPM, the rotor energy has been assumed constant for this study. By deriving equation (5) with respect to time, it is possible to express the power equation:

$$\Delta P = \frac{dE}{dt} = mV\frac{dV}{dt} + mg\frac{dh}{dt} \quad (6)$$

According to Zuang [47], the rotor power required in forward flight is given by the sum of parasite power, induced power, rotor blade profile power, compressibility power, stall power, and climb power.

$$P_{req,rot} = \frac{1}{2}A_f\rho V_x^3 + TV_i + 0.125\delta bcR(1+4.6\mu^2)\rho(\Omega R)^3 + \\ + \rho\Omega^3\pi R^5\Delta M^3[0.0033 - \Delta M(0.022 - 0.11\Delta M)] + \quad (7) \\ + \kappa^{1.5}(t_c - t_{cdiv}) + mgV_y$$

Power can be expressed by the simplified equations by McCormick [48] for horizontal flight.

$$P_x = P_{x,o} + \frac{1}{2}\cdot\frac{(m\cdot g)^2}{\rho\cdot A_f\cdot V_x} + \frac{1}{2}\cdot\rho\cdot C_{D,x}\cdot A_f\cdot V_x^3 \quad (8)$$

and for vertical flight

$$P_y = V_y\cdot\left(mg + \frac{1}{2}C_{D,y}\cdot A_t\cdot\rho\cdot V_y\right). \quad (9)$$

Total power is consequently

$$P_{tot}=P_x+P_y \quad (10)$$

The total power required is obtained by rotor power and overall efficiency factor η is

$$P_{req,tot} = \eta\cdot P_{req,rot}. \quad (11)$$

## OPTIMIZATION OF HELICOPTER EQUATIONS

By equations (4) and equations (8) and (9), it is possible to produce a preliminary abstract optimization of a theoretical system that can act as according to those equations and then performing the same operations that a helicopter does. Starting from the optimization of the system of forces that may be produced by a hypothetical flying vehicle that can act as a helicopter it is immediate to observe that the best conditions are the ones that allow minimizing thrust or moment in any direction.

### Analysis of forces and moments

Equation of rotation around vertical axis shows clearly that avoidance of the propulsion system with a vertical axis of rotation allows making null the rear rotor moment. Equation of rotation around z-axis shows that it can minimize thrust by an aerodynamic system that can grant an adequate momentum by mean of aerodynamic lift by wings or ailerons. A similar conclusion is obtained by the equation of vertical motion. The vertical thrust $T_y = T\cos\phi$ lowers by both increasing the vertical lift by aerodynamic surfaces and lowering the vertical drag. The equation of horizontal motion shows that the minimization of horizontal thrust requires the minimization of horizontal drag.

### Energetic model

Further analysis will relate to the energy analysis of the system. The power equation found in traditional bibliography, which have been cited in the preceding paragraph, can be improved by a more accurate analysis according to Trancossi [4, 9, and 10].

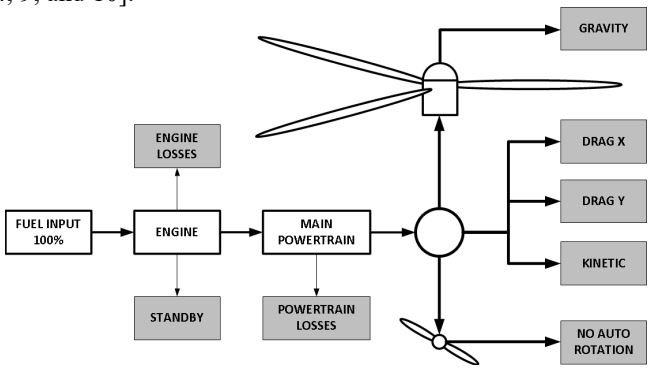


**Figure 12. Energy dissipations in a helicopter**

Figure 12 shows energy losses for the moving vehicle. A schema of the powertrain indicating the different losses is provided in Figure 2. Losses depend on the flight condition in which the helicopter operates.

For simplicity, the model will be developed neglecting minor energy components and assuming that vertical lift force is mostly produced by propulsion and not by aerodynamic appendices. Applying this model to the helicopter, it is evident that the energy components that have to be considered are more complex with respect to other transport modes. They are:

$$E_{K,x} = \frac{1}{2}mv_x^2; E_{K,y} = \frac{1}{2}mv_y^2$$

$$L_{T,x} = \int_0^{t_{tot}} T_x v_x dt; L_{T,y} = \int_0^{t_{tot}} T_y v_y dt$$

$$L_{D,x} = \int_0^{t_{tot}} \left( \frac{1}{2} C_{D,x} \rho A v_x^2 \right) v_x dt; E_{D,y} = \int_0^{t_{tot}} \left( \frac{1}{2} C_{D,y} \rho A v_y^2 \right) v_y dt$$

$$E_{P,y} = mgh$$

$$E_{R,p} = \frac{1}{2} I_p \Omega_p^2; E_{R,r} = \frac{1}{2} I_r \Omega_r^2$$

The evaluation of exergy needs for moving can be performed by equation (12)

$$Ex_{service} = m_{tot} \left( gh + \frac{1}{2} v_{\max,x}^2 + \frac{1}{2} v_{\max,y}^2 \right) + \frac{1}{2} C_{D,x} A_x \rho_{air} v_{av,x}^3 t_x + \frac{1}{2} C_{D,y} A_y \rho_{air} v_{av,y}^3 t_y + \frac{1}{2} I_p \Omega_p^2 + \frac{1}{2} I_r \Omega_r^2 \quad (12)$$

Equation (12) can be divided into two equations, one related to the vehicle and one to the payload:

$$Ex_{veh} = m_{veh} \left( gh + \frac{1}{2} v_{\max,x}^2 + \frac{1}{2} v_{\max,y}^2 \right) + \frac{1}{2} C_{D,x} A_x \rho_{air} v_{av,x}^3 t_x + \frac{1}{2} C_{D,y} A_y \rho_{air} v_{av,y}^3 t_y + \frac{1}{2} I_p \Omega_p^2 + \frac{1}{2} I_r \Omega_r^2 \quad (13)$$

$$Ex_{pay} = m_{pay} \left( gh + \frac{1}{2} v_{\max,x}^2 + \frac{1}{2} v_{\max,y}^2 \right) \quad (14)$$

It can be also possible to write express energy losses of engine and power train:

$$Ex_{vehicle} = Ex_{fuel} - L_{engine} - L_{standby} - L_{Powertrain} \quad (15)$$

Equations (12), (13) and (14) allow analysing the performances in service conditions during operations of the vehicle. In particular, equation (13) and (14) allows expressing the energy consumption required for moving the vehicle and the payload.

## Energy optimization

The above model allows an effective energetic optimization of a vehicle that virtually can operate according to the same physical laws that applies to a helicopter. By the preliminary evaluations made on forces and moments it can be possible to perform a preliminary minimization of the terms that appear in the energy balance:

$$Ex_{service} = m_{tot} \left( \frac{1}{2} v_{\max,x}^2 + \frac{1}{2} v_{\max,y}^2 \right) + \frac{1}{2} C_{D,x} A_x \rho_{air} v_{av,x}^3 t_x + \frac{1}{2} C_{D,y} A_y \rho_{air} v_{av,y}^3 t_y \quad (16)$$

It simplifies during horizontal flight:

$$Ex_{service} = m_{tot} \left( \frac{1}{2} v_{\max,x}^2 \right) + \frac{1}{2} C_{D,x} A_x \rho_{air} v_{av,x}^3 t_x$$

Equation (16) can describes the system behaviour of a vehicle during horizontal flight and lift operations. It could not describe the energy equilibrium during vertical lift and during hovering. Those operations can be described by equation (17)

$$Ex_{service,y} = m_{tot} \left( gh + \frac{1}{2} v_{\max,y}^2 \right) + \frac{1}{2} C_{D,x} A_x \rho_{air} v_{av,x}^3 t_x + \frac{1}{2} C_{D,y} A_y \rho_{air} v_{av,y}^3 t_y \quad (17)$$

It is necessary to consider the component that relates to horizontal drag, because it is not frequent to be in the condition of ideal calm air. However, this component can be neglected with very low airspeeds around the vehicle.

## Preliminary analysis

It is evident by the above considerations that helicopter is the less energy efficient among the above-considered propulsion systems and vehicles at least in horizontal flight. It is also evident that none of the possible solution seen before allows replicating helicopter operations, at least is they are used in known configurations, with the only exception of tilting rotors and cyclorotoidal propulsion.

Tilting rotors, even if they seem growing, present large safety related problems, stability problems and has demonstrated diffused operative limitations. Cyclorotoidal propellers ensure an effective replication of typical manoeuvres that helicopters can do such as inversion of direction and static hovering. Otherwise the fragility of this system or the necessity of increasing dimensions and weights to avoid this problem could constitute a dangerous showstopper, which can delay or making impossible its implementation on the aircrafts. In particular, the necessity to work at low speeds to reduce the fatigue effects and vibrations is a potential problem for its competitiveness with respect to propelled wings. On the other side today known designs of propelled wings and Magnus effect enhancers ensure high affordability but could not emulate the operative flexibility of helicopters. Other systems, such as jet wing discharge systems, have the same limitations of propelled wings. ACHEON is instead just a nozzle, which can have large benefits on vehicle manoeuvrability and reduction of take off, and landing spaces, but it has not the capability of being itself a system with the capability of emulating helicopters. An effective future solution that can emulate helicopter flexibility and operative capability needs designing new solutions by scratch which can resemble known technologies in a specific way that can ensure the required operative results with a much higher energy efficiency with respect to helicopters over the entire lifecycle.

Any optimized solution must respond to the optimized equations (12), (13) and (14) in any flight conditions. To allow a preliminary conceptual design of such a vehicle, if it is possible, it is necessary to start from considering the optimized forces and energy conditions that it must satisfy over different flight condition and missions. Those conditions in terms of force can be represented conceptually on a preliminary diagram and then they can be considered by an accurate operative and energetic analysis. The schematization of optimal force condition is represented in Figure

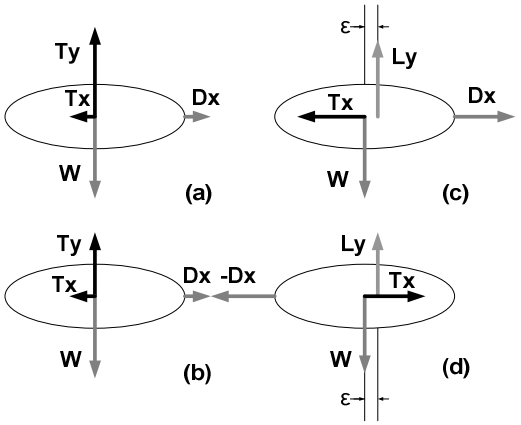


**Figure 13. Representation of the forces acting on the ideal vehicle: (a) vertical upward movement; (b) vertical downward movement; (c) horizontal movement; (d) horizontal backward movement.**

Looking at the conditions that have been represented into Figure 13, it is clear that hovering in calm air can be represented by (a) and (b) with $D_x=T_x=0$. It is also evident that ideal condition correspond to a null distance between $L_y$ and $W$. Any system which satisfy those conditions must have a symmetric distribution of loads during horizontal flight including aerodynamic ones (lift Ly). In particular, during stationary hovering in calm air it must have only a vertical component of forces. It is then clear that none of the propulsion concepts presented can satisfy this condition.

## POSSIBLE SOLUTIONS

Considering that traditional wing have lift over drag ratios in the area of 5 to 7, propelled wings can reach by the induced increase of the velocity in the higher part of the wing, higher attraction effect on surrounding fluid and Coanda adhesion values of lift over drag that overcome 13 also at very low velocities. The ideal solution to the problem could then be a complete redesign of actual propelled wings and of actual propelled wing powered aircrafts to meet the above performance parameters without significant losses in term of performances. In particular a more flexible propelled wing concept that can work with pass-through fans but also other propulsion systems is expected to be produced. This solution, if could be found could be the more advanced one in this direction which have been ever seen and in particular the only one that could really outclass the operational flexibility of helicopters with much higher performances with respect to any existing solution.

## A REVERSIBLE SYMMETRIC PROPELLED WING CONCEPT

Taking into consideration the results obtained by Bejan [49, 50] the design of the proposed quad rotor can be further optimized ensuring a better flow of air and a better positioning of the rear rotors which still presents some operative limitations, because they are disturbed by frontal ones. The conceptual design has been performed by an effective constructal optimization [51 - 53] of the system. It is then necessary to consider each subsystem defining the components that allow reaching the best system performance on the selected quantities. The above analysis has produced an effective design of an innovative breakthrough aircraft, which has innovative features such as a symmetric shape with symmetric wings and propulsion fitted inside the wings. The energetic model of the system shows clearly that weight is the critical element that conditions the performance of the system both in terms of absolute performances and in terms of energetic performances that means capability of maintaining the system in flight. Such considerations force to choose the components assuming the weight for performances as the main criteria for dimensioning.

This system allows producing the aircraft design, which is presented in Figure 14. This new propelled wing concept is symmetric with respect a vertical axis and has two symmetric openings on the top surface, which can act alternatively as air inlet or outlet of the propulsion system, depending on the direction of motion. It is characterized by having propulsion with air intake and outlet in the upper part of the wing. Figure 15 shows the behaviour of the wing showing velocity and pressure behaviour with respect to the one of the same shaped wing without inlet and outlet. .

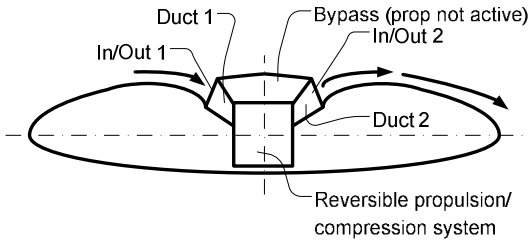


**Figure 14. Propelled wing and core parts**

It is expected that the above wing configuration can take advantage of different propulsion methods that ensure the possibility of reversible inversion.

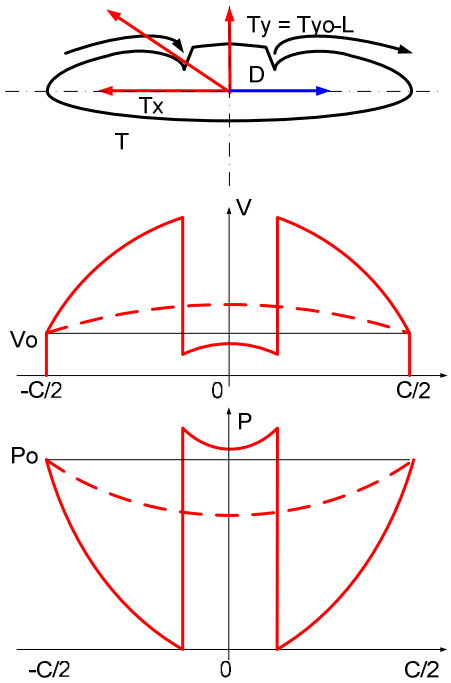


**Figure 15. Theoretically expected behaviour as a function of the position.**

The inversion can be ensured by both a reversible propulsion system (counter rotating fans, variable pitch fans, pass-through fans, etc.) and fluiddynamic systems that allows inverting the direction of aspiration and propulsion of any traditional system, which is capable of producing a fluiddynamic thrust. From Figure 15, it is evident that the wing can be modelled in order to reach a lift, which is much higher with respect to the one that is produced by the same wing.

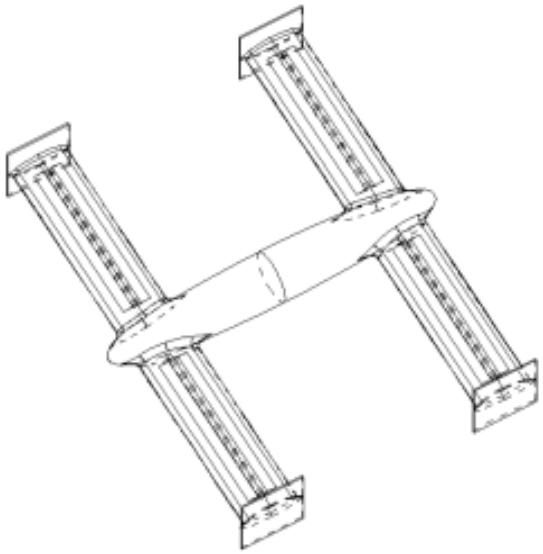

**Figure 16. Preliminary conceptual design of the aircraft**

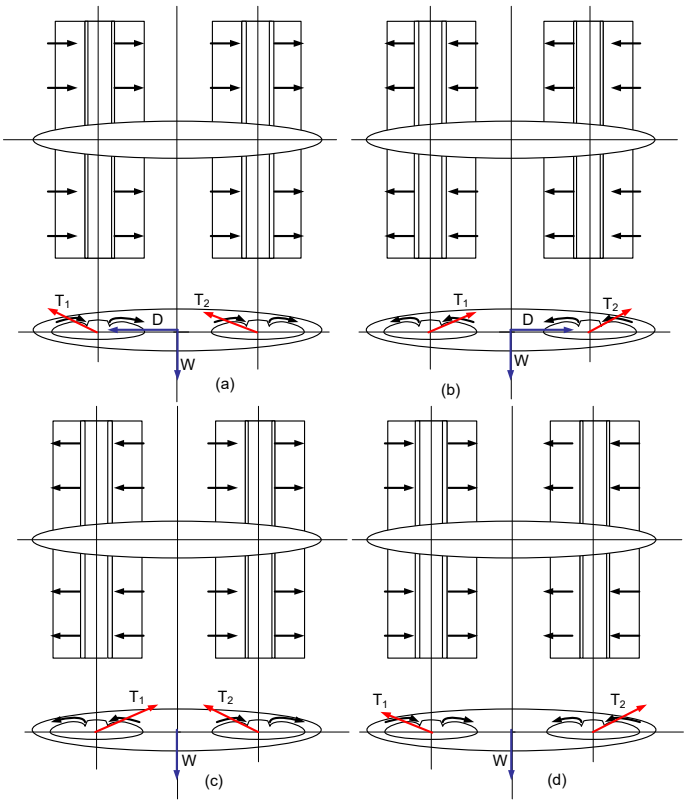


**Figure 17. Fight modes**

It is evident that if two identical wings of this kind are placed on a fuselage (Figure 16) they can ensure forward flight by using the propulsion in the same direction (Figure 17/a), can invert the direction of flight by reducing the speed and inverting the direction of the thrust on both wings (Figure 17/b). Static hovering require that the wings have opposite propulsive directions with same magnitude, when they are in calm air (Figure 17/c) or in the way to produce a difference in thrust that allows facing the action of the wind (Figure 17/d).

## NUMERICAL VERIFICATION OF THE HYPOTHESIS

From Figure 15, it is evident that the wing can be modelled in order to reach a lift, which is much higher with respect to the one that is produced by the same wing. A large CFD campaign has been produced to evaluate the benefits of the proposed propelled wing. Tested sample geometry has been presented in Figure 18. The problem has been approached by two CFD codes: Ansys Fluent [54], figures 19 and 20, and EasyCFD [55], figures 21 and 22.

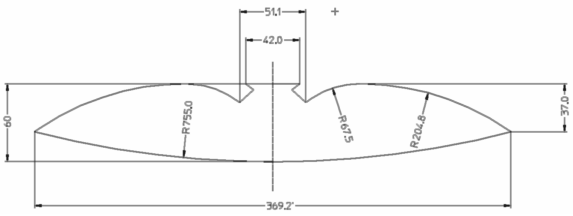


**Figure 18. Tested sample geometry**

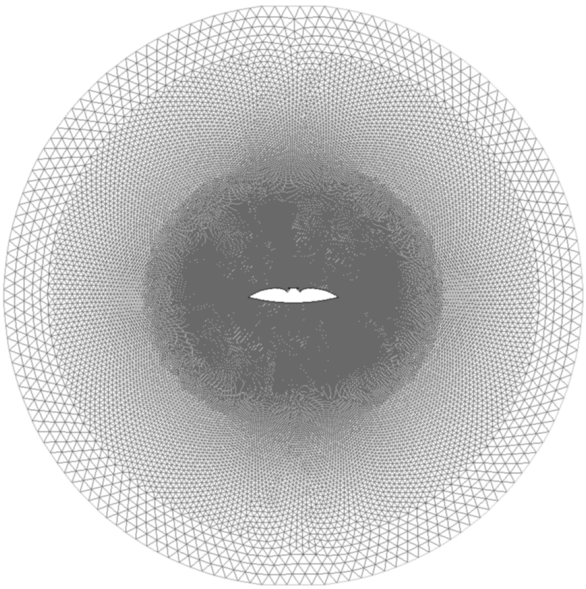

**Figure 19. Mesh used by Ansys Fluent**

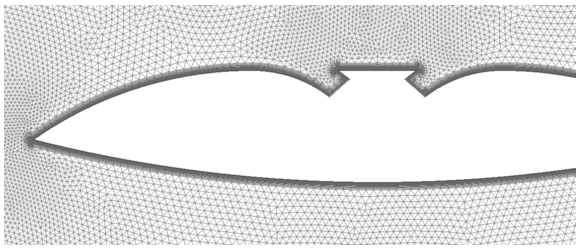

**Figure 20. Sample of the mesh realized by Gambit using Boundary Layer**

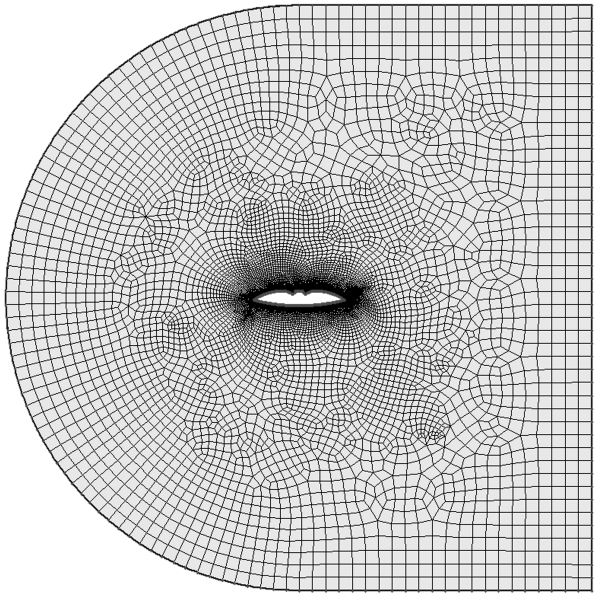

**Figure 21. Quad unstructured mesh realized by EasyCFD**

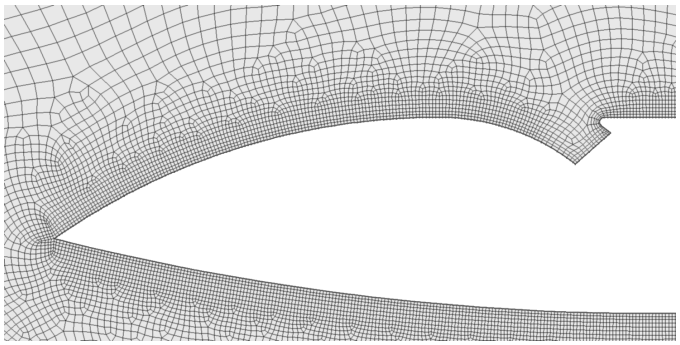

**Figure 22. Clean quad mesh realized by EasyCFD**

## Conditions for CFD analysis

The following conditions have been defined for CFD analysis:

1. $P = P_{atm}$ (0 m) = 101325 Pa
2. $V_0$ = 2.5; 5; 10; 15 m/s
3. Turbulence models used:
   Spalart-Almaras (for preliminary tests)
   kΩ-SST (for accurate testing)
4. propulsion mass flow inlet is equal to outlet.

## Mesh convergence analysis

Convergence analysis had to be different between the two codes. It has been developed by starting from a common basis even if different mesh accuracies has allowed to reach an effective convergence for the two codes, because of the different nature of the meshes. The main reference for this analysis has been the Policy Statement by ASME Journal of Fluid Mechanics [56]. The specific nature of the problem that involves Coanda adhesion, fluid attraction and aerodynamic drag and lift has forced to a deeper investigation, by considering a wide set of supplementary sources [57-60].

The following procedure describes the adopted grid convergence study. The flow field is computed on different grids, each with increasing number of grid points in the i and j coordinate directions as the previous grid. No analysis in k coordinate direction is necessary being a problem that can be described by a 2D grid, at least for a preliminary evaluation. The table below indicates the grid information and the resulting pressure recovery computed from the solutions.

Because of using two different CFD codes, two convergence analyses have been realized, one for Fluent and one for Easy CFD. Each solution was properly converged with respect to iterations. The column indicated by "spacing" is the spacing normalized by the spacing of the finest grid on the propelled wing surface.

Figure 23 shows the plot of pressure recoveries with varying grid dimensions. As the grid spacing reduces, the pressure recoveries approach an asymptotic zero-grid spacing value. It can be calculated the order of convergence, which results $L_{conv,Fluent}=1.2055$ or $L_{conv,EasyCFD}=1.1012$, which are lower than the theoretical order of convergence is $L_{th,conv}=2.0$.

**Table 1. Convergence analysis**

| Grid | Normalized Grid Spacing | Inlet air speed | Propulsion induced air speeds | Lift force (Fluent) | Lift force (EasyCFD) |
|---|---|---|---|---|---|
| | (mm) | (m/s) | (m/s) | (N) | (N) |
| 1 | 3 | 5 | 10 | 2.1952 | 2.1953 |
| 2 | 6 | 5 | 10 | 2.1843 | 2.1843 |
| 3 | 12 | 5 | 10 | 2.1601 | 2.1607 |
| Lift convergence ratio $L_{conv}$ | | | | 1.2055 | 1.1013 |
| Theoretical lift $L_{rh}$ | | | | 2.2043 | 2.2049 |
| Grid Convergence Index GCI1,2 (FS=1.25) | | | | 0.5286% | 0.5468% |
| Grid Convergence Index GCI2,3 (FS=1.25) | | | | 1.1550% | 1.1790% |

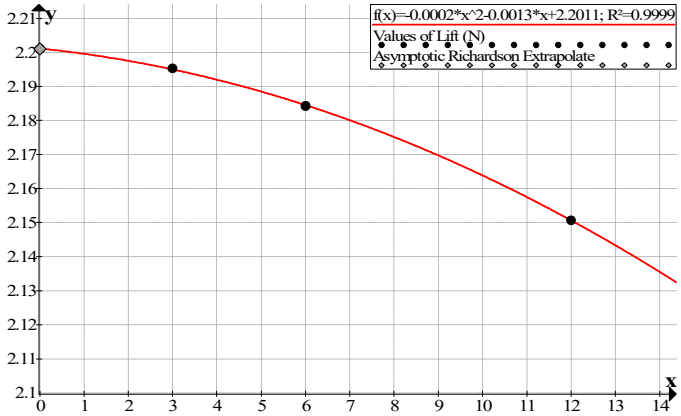


**Figure 23. Graph of values used for fluent mesh convergence**

The difference is most likely due to grid stretching, grid quality, non-linearity in the solution, presence of shocks, turbulence modelling, and perhaps other factors. Richardson extrapolation using the two finest grids allow obtaining an estimate of the value of the Lift recovery at zero grid spacing,

$L_{rh} = 2.2043$

This value is also plotted on Figure 23.

The grid convergence index for the fine grid solution can now be computed. A factor of safety is used since three grids were used to estimate p. The GCI for grids 1-2 and 2-3 are:

$GCI_{1,2} = 0.5286\%$

$GCI_{2,3} = 1.1550\%$

We can now check that the solutions were in the asymptotic range of convergence,

$Fluent = 0.5286/(2^{1.2055}\ 1.1550) = 2.1852.$

$EasyCFD = 0.5468/(2^{1.1013}\ 1.1790) = 2.1562.$

It means that the solutions are well within the asymptotic range of convergence.

Based on this study it is possible to conclude that the 3 mm grid seems accurate enough and that $L_{th} \cong 2.2$ with an error band up to 1%. Then this grid dimension on the surface has been adopted for both the systems because it is completely acceptable for this preliminary evaluation.

## CFD results

The results have been inline between the two numerical codes. It is important. Some samples of solution have been reported in figures (24) to (27).

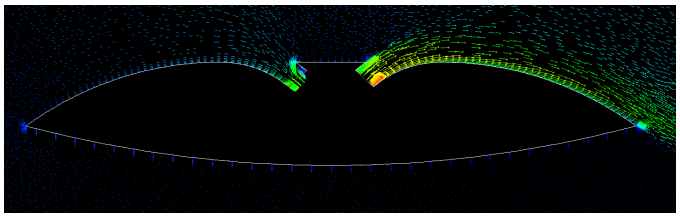

**Figure 24. Sample of Velocities (Fluent)**

**Figure 25. Sample of pressure (Fluent)**

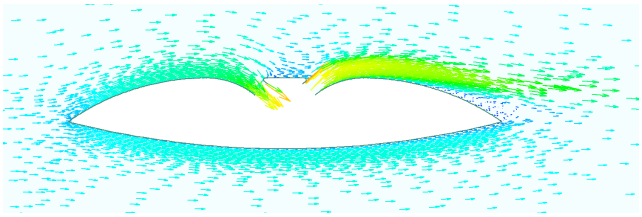

**Figure 26. Sample of Velocities (Easy CFD)**

The results appear interesting and for the specific wing they have reported in Figure 28 (Lift) and 29 (Drag).

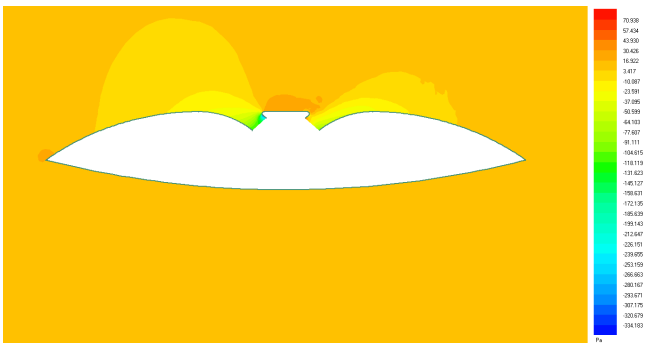

**Figure 27. Sample of Pressure Mapping (Easy CFD)**

Several CFD simulations at different angles of attach have been produced also, with consistent increase in term of Lift. Evaluation of Lift and Drag variations with angle of attach is currently under development considering both the wing alone and the aircraft.

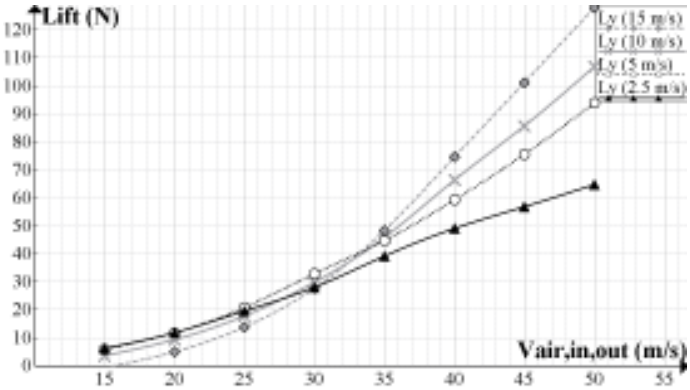


**Figure 28. Lift at different air speeds (angle of attach equal to 0)**

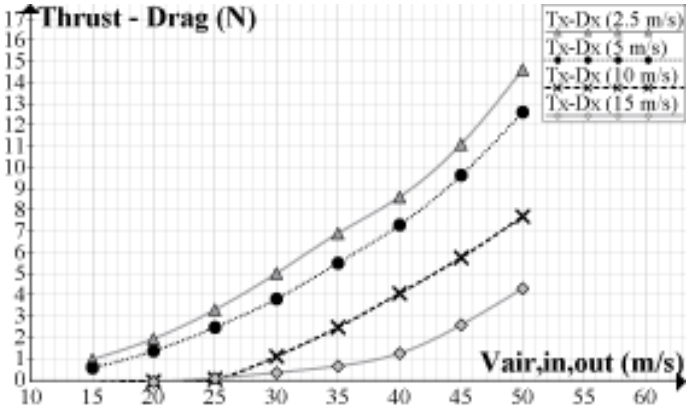


**Figure 29. Thrust - Drag at different air speeds (angle of attach equal to 0)**

Evaluation of the symmetric wing with the same profile has been necessary to produce comparable results with competitors such as FanWing. This case has been evaluated at different air speeds,

The tested wing profile geometry is presented in Figure 30.

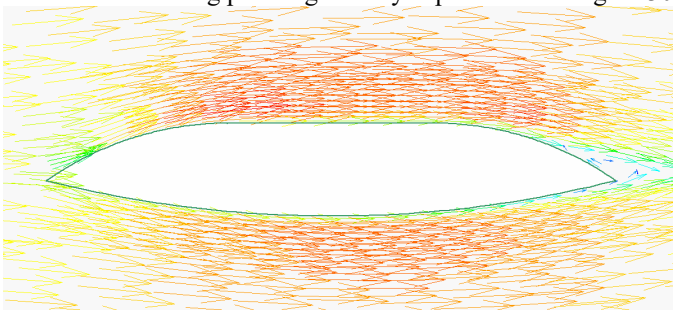

**Figure 30. Profile of traditional wing profile tested with velocity vectors.**

Plotting the ratio between Lift of the powered wing and corresponding wing results appears outstanding and they have been plotted in Figure 30.

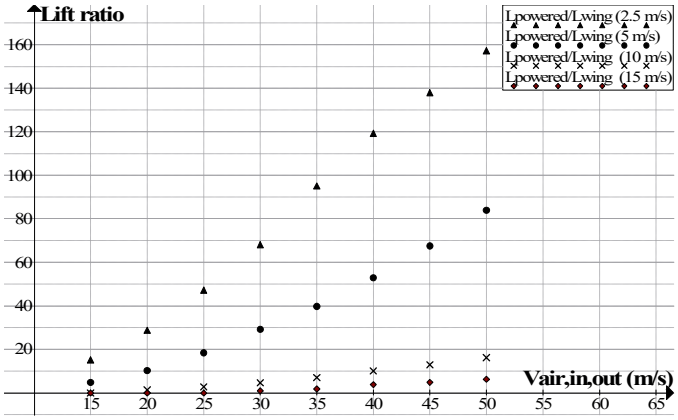


**Figure 31. Ratio between propelled wing and corresponding wing profile**

The results in figure 31 show clearly a very high increase in lift at very low speed that is the main capability that this wing ensures. It also shows that the gain increases with the propulsive kinetic energy that the propelling system can ensure to the air. It then states that propelling wing system are much more performing when coupled with high speed propulsion systems. It also shows that at the same propulsion air speeds the advantages reduce with increasing external air speeds.

## ENERGY BALANCE

The obtained results allow producing an effective energy balance of the same vehicle against a helicopter in different flight conditions. Vehicles compared are a traditional helicopter with high performances and a symmetric wing aircraft. The comparison has been produced at Small UAV scale. Data about the two vehicles are reported in Table 2. Table 3 reports the key components of the symmetric wing UAS according to the preliminary design presented in Figure 16 and 17.

**Table 2. Technical specification of vehicles**

| | units | Helicopter | Symmetric wing |
|---|---|---|---|
| Length | mm | 750 | 1200 |
| Width | mm | 246 | 1200 |
| Height | mm | 430 | 350 |
| Main Blade Length | mm | 400 | - |
| Main Rotor Diameter | mm | 950 | - |
| Flying Weight Approx | kg | 2.75 | 2.75 |
| Payload | kg | 0.5 | 0.5 |

After an accurate evaluation it has been identified a material for the aircraft body. It is high quality Depron [20, 21] with a density of 40 kg/m³, compressive strength 0.10 MPa (compression 10°) and a tensile stress of 1.30 MPa in main direction and 0.70 MPa in transversal direction. High quality ABS injection grade (density 1.05 kg/dm3) can be used for minor parts with low structural loads. Similar weights can be

easily assumed by carbon fibres components, which could allow higher resistance but has higher costs.

**Table 3. Technical data and weights for symmetric wing design.**

| Component | Unitary mass | Num. | Total mass |
|---|---|---|---|
| | g | - | g |
| Structure | 540 | 1 | 540 |
| Wing pass though fans | 130 | 4 | 520 |
| Heli Motors 1555 rpm/(min Volt) | 175 | 4 | 700 |
| 35A Brushless Programmable ESC w/BEC Speed control | 13 | 4 | 52 |
| Receiver V8FR-II 2.4Ghz 8CH (HV) | 10 | 1 | 10 |
| LiPo Battery 25C 7800mAh 3-Cell/3S 11.1V | 530 | 1 | 530 |
| Cabling and accessories | 120 | 1 | 100 |
| | | **Total mass** | **2352** |

Energy balance is produced by considering equation (16) and (17). A reference profile mission is defined in Figure 32.

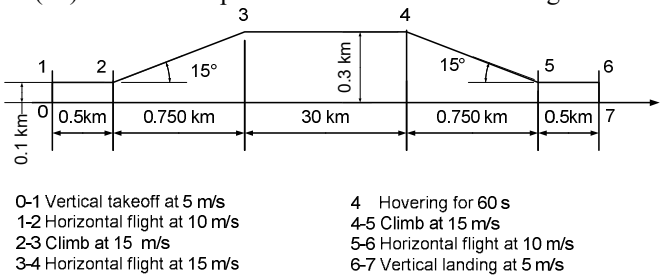


**Figure 32. Mission Profile**

Both helicopter and symmetric propelled wing aircraft have been assumed 2.75 kg at takeoff. The results from wind gallery testing and the estimation of the thrust of a single propeller allow an effective comparison with helicopter. Assuming the same climb speed (2.5 m/s differs in reason of the propeller areas.) and the same thrust nearly equal to weight, it is possible to verify that the propulsive efficiencies are quite different. Results for different flight condition can be reassumed in Table 4. The values for helicopter in table 4 have been evaluated according to the equations in Annex 1, equation (15) and (16). They clearly appear inline with Zuang [6]. Specific values, which can apply to the specific simplified version for propelled symmetric wing aircraft concept, have been evaluated according to CFD results and formula (15) and (16) in their simplified forms. Propulsion system has been evaluated assuming losses in terms of electrical energy of 5% for helicopters and 10% for symmetric propelled wing aircraft.

Results allow demonstrating preliminarily the much higher energy efficiency of the proposed aircraft concept even in a mission profile with important hovering and vertical flight operations.

**Table 4. Comparison of extimated energy performances between a helicopter and a propelled wing aircraft**

| | | *Air speed* | *Lenght* | *Height change* | *Time* | *Helicopter* | | *Propelled wing* | |
|---|---|---|---|---|---|---|---|---|---|
| | | | | | | *Power* | *Energy* | *Power* | *Energy* |
| | | (m/s) | (m) | (m) | (s) | (W) | (kJ) | (W) | (kJ) |
| Vertical take off | P0-1 | 5 | 100 | 100 | 20.0 | 1750 | 35.0 | 2950 | 59.0 |
| Horizontal flight | P1-2 | 10 | 500 | 0 | 50.0 | 1300 | 65.0 | 450 | 22.5 |
| Climb | P2-3 | 15 | 772.5 | 200 | 51.5 | 1400 | 72.1 | 500 | 25.8 |
| Horizontal Flight | P3-4 | 15 | 3000 | 0 | 200.0 | 1300 | 260.0 | 450 | 90.0 |
| Hovering | P4 | 0 | 0 | 0 | 30.0 | 1750 | 52.5 | 2950 | 88.5 |
| Descent | P4-5 | 15 | 772.5 | -200 | 51.5 | 1400 | 72.1 | 500 | 25.8 |
| Horizontal flight | P2-4 | 10 | 500 | 0 | 50.0 | 1300 | 65.0 | 450 | 22.5 |
| Vertical landing | P0-3 | 5 | 100 | -100 | 20.0 | 1750 | 35.0 | 2950 | 59.0 |
| ***Average values*** | | ***12.1*** | | | | ***1388*** | | ***831*** | |
| ***Total significant values*** | | | ***5745*** | ***0*** | ***473*** | | ***656.7*** | | ***393.0*** |

## CONCLUSIONS

After a general presentation of the competitors of helicopters and their pro and contra with respect to helicopter, this paper has analyzed the genesis of a new aircraft concept that aims to rival against helicopter by an effective energy analysis of the operations of the helicopter. The results has been a breakthrough aircraft concept which take advantage of a an innovative propelled wing. This wing is based on a revolutionary concept and a symmetric shape, which allow having a reversible behaviour. This concept has been explored by a preliminary CFD activity, even if rigorous which ha allowed determining the performances for a unitary length one in terms of horizontal and vertical thrust, showing very high

over-lift possible even at very low speeds. It has been explored its performance in the range of very low speeds (airspeeds from 2.5 to 15 m/s) that is outside the traditional speed-range of aircrafts. By the obtained results it has been clearly possible to explore the superior energy performances of this aircraft at small UAS scale. It clearly demonstrates the superior energetic performance of this aircraft concept in small-scale size, with respect to the helicopter. Considering the assumed mission profiles that includes vertical take off, landing, and hovering, it has been possible to demonstrate a theoretical reduction with respect to helicopter around 40%.

The breakthrough propulsion concept and the internal architecture of the wing, which are a fundamental part of this innovative propelled wing concept cannot be disclosed at this level because of patenting related issues.

## REFERENCES


1. Wood T L, Livingston C L, An energy method for prediction of helicopter manoeuvrability AD Report, ADA021266, 1971.
2. Johnson W., Helicopter theory Dover Publications: New York, 1994.
3. Kiwan A R. Helicopter performance evaluation (HELPE) computer model, AD Report AD-A284 319/1, 1994.
4. Trancossi M., What price of speed? A critical revision through constructal optimization of transport modes., International Journal of Energy and Environmental Engineering pp 1-24, First online, 2015.
5. VV.AA., “Helicopter flight handbook”, Federal Aviation Authority, US Department of transportation, 2012.
6. Zhuang N, Xiang, J. et al., "Calculation of helicopter maneuverability in forward flight based on energy method", Computer Modelling & New Technologies, 18(5) 50-54, 2014.
7. Dewulf J, and Van Langenhove H., “Exergetic material input per unit of service (EMIPS) for the assessment of resource productivity of transport commodities”. Resources Conservation and Recycling. 38(2), Pages: 161–174 (2003).
8. Gong M., Wall G., “On exergy and sustainable development—Part 2: Indicators and methods”, Exergy, An International Journal, Volume 1, Issue 4, 2001, P. 217–233.
9. Trancossi M., A response to industrial maturity and energetic issues: a possible solution based on constructal law, European Transport Research Review, January 2015, 7:2, 2015.
10. Trancossi, M., et al., "A new aircraft architecture based on the ACHEON Coanda effect nozzle: flight model and energy evaluation". European Transport Research Review, 8 (2), 11 (1)-11 (21), 2016.
11. Whittle, R., “The Dream Machine: The Untold History of the Notorious V-22 Osprey”, Simon and Schuster, pp.464, 2010;
12. Seck, H. H., “Billows of Dust, a Sudden 'Pop' and an Osprey Falls from the Sky”, Military.com, 2016, http://www.military.com/daily-news/2016/01/29/billows-of-dust-a-sudden-pop-and-an-osprey-falls-from-the-sky.html
13. VV. AA. “Voith Schneider Propeller,” World-Wide Web document, http ://en.wikipedia.org/wiki/VoithSchneiderPropeller, Nov 28, 2010.
14. VV. AA., “Voith Schneider Propeller,” World-Wide Web document, http ://www.renewbl.com/2010/07/16/voith − turbo − supplying − propellers − for − two − jack − up − vessels.html, July 16, 2010.
15. Leger, J., Pascoa, J. C. ,and Xisto, C. M., “Analytical Modeling of a Cyclorotor in Forward Flight,” in SAE 2013 AeroTech Congress & Exhibition, 2013.
16. Leger, J., Pascoa, J. C. ,and Xisto, C. M., “Parametric Design of Cycloidal Rotor Thursters,” in Proceedings of ASME 2013 International Mechanical Engineering Congress & Exposition IMECE 2013, 2013.
17. Trancossi, M., Dumas, A., Xisto, C., Pascoa, J. et al., "Roto-Cycloid Propelled Airship Dimensioning and Energetic Equilibrium," SAE Technical Paper 2014-01-2107, 2014, doi:10.4271/2014-01-2107.
18. Massey H., “Means and method for increasing the magnus effect”, Pat. US2344515 A, 1941.
19. Hirschel E., Prem H., Madelung G. et al., “Aeronautical Research in Germany: From Lilienthal Until Today”, Volume 147, 2004.
20. Coanda H., “Jet Propelled Aircraft”, Pat. US2946540 A, 1948.
21. Goembel P., “Jet propelled airplane with wing discharge slot”, Pat. US2479487, 1946.
22. Bradbury D., and Meyer C., “Wing-mounted jet-propulsion system with controllable discharge outlet”, Pat. US2420323 A, 1943.
23. Kummer J., Dang T, “Cross-flow fan propulsion system”, Pat. US20060266882, 2006.
24. Peebles P. W., “Aircraft with aerodynamic lift generating device”, Pat. US8448905, 2006.
25. Baffigi F., Dumas A., Giuliani I., Madonia M., and Trancossi M., (2014) "Ugello capace di deviare in modo dinamico e controllabile un getto sintetico senza parti meccaniche in movimento e relativo sistema di controllo", Patent IT 0001406404, Deposito RE2011A000049, Filling date July 01, 2011, Publication date September 30, 2011, approved on February 21, 2014.
26. Baffigi F., Dumas A., Giuliani I., Madonia M., and Trancossi M., (2014), "Nozzle capable of deviating a synthetic jet in a dynamic and controllable manner with no moving mechanical parts and a control system thereof", PTC Patent WO2013005132 A1, Publication date Jan 10, 2013, Filing date Jun 25, 2012, Priority date Jul 1, 2011, Published also as EP2726213A1, US20140191059
27. Trancossi, M., “An Overview Of Scientific And Technical Literature On Coanda Effect Applied To Nozzles”, SAE Technical Papers N. 2011-01-2591, Issn 0148-7191, 2011;

28. Trancossi M. and Dumas A., (2011) “ACHEON: Aerial Coanda High Efficiency Orienting-Jet Nozzle ”, Sae Technical Papers N. 2011-01-2737, Issn 0148-7191.
29. Trancossi, M., Dumas, A., (2011) “Coanda Syntetic Jet Deflection Apparatus And Control”, SAE Technical Papers N. 2011-01-2590;
30. Trancossi, M., Dumas, A., (2011) “ACHEON: Aerial Coanda High Efficiency Orienting-Jet Nozzle ”, Sae Technical Papers N. 2011-01-2737.
31. Páscoa, J.C., Brójo F. M. P., and Monteiro J. M. M., "Numerical Simulation of Magneto-plasma Thrusters for Aerospace Propulsion Using and MHD Formulation", Paper O-7.2, Proc. 14th International Conference on Emerging Nuclear Energy Systems, Instituto Tecnológico e Nuclear, 6 pgs, (2009).
32. Trancossi, M., Dumas, A., and Vucinic, D., "Mathematical Modelling of Coanda Effect," SAE Technical Paper 2013-01-2195, doi:10.4271/2013-01-2195, 2013.
33. Subhash, M. and Dumas, A., (2013) "Computational Study of Coanda Adhesion Over Curved Surface," SAE Int. J. Aerosp. 6(1):260-272, doi:10.4271/2013-01-2302.
34. Dumas, A., Subhash, M., Trancossi, M., and Marques, J.P., (2014) "The influence of surface temperature on Coanda effect", Energy Procedia Vol. 45, pp. 626-634
35. Dumas, A., Pascoa, J., Trancossi, M., Tacchini, A., Ilieva, G., and Madonia, M., "Acheon project: A novel vectoring jet concept", Proc. ASME. 45172; Volume 1: Advances in Aerospace Technology: 499-508, IMECE2012-87638, 2012.
36. Pascoa, J. C., Dumas, A., Trancossi, M., Stewart, P., and Vucinic, D., "A review of thrust-vectoring in support of a V/STOL non-moving mechanical propulsion system" Cent. Eur. J. Eng., 3(3), pp. 374-388, (2013).
37. Das, S.S., Abdollahzadeh, M., Pascoa, J. C., Dumas, A., and Trancossi, M., “Numerical modelling of Coanda effect in a novel propulsive system”, Int. Jnl. of Multiphysics, Volume 8 · Number 2, pp. 181-201, 2014
38. Trancossi, M., Dumas, A., Das, S. S., and Páscoa, J. C., (2014) “Design Methods of Coanda nozzle with two streams”, INCAS Bulletin, Volume 6 (1), Pages 83-95, ISSN 2066-8201, doi: 10.13111/2066-8201.2014.6.1.8
39. Trancossi M, Subhash M., Angeli D., “Mathematical modelling of a two streams Coanda effect nozzle.” ASME Int. Mech. Engg. Conf. and Exhibition, paper no. IMECE2013-63459; 2013.
40. Trancossi, M., “Design of ACHEON Thrust and Vector Propulsion System,” SAE Technical Paper 2015-01-2425, 2015, doi:10.4271/2015-01-2425.
41. Abdollahzadeh M., and Pascoa J., Modified Split-Potential Model for Modelling the Effect of DBD Plasma Actuators in High Altitude Flow, Control Current Applied Physics, (2014).
42. Abdollahzadeh, M., Páscoa J.C., and Oliveira P.J., (2014) "Two-dimensional numerical modelling of interaction of micro-shock wave generated by nanosecond plasma actuators and transonic flow", Journal of Computational and Applied Mathematics, Volume 270, pp. 401
43. Xisto C, Páscoa J, and Oliveira P, "Modelling plasma flow on a self-field MPD thruster using a PISO based method", 44th AIAA Plasmadynamics and Lasers Conference, San Diego, USA, (2013).
44. Cen Z., Smith T., Stewart P., and Stewart J, "Integrated flight/thrust vectoring control for jet-powered unmanned aerial vehicles with ACHEON propulsion", Proceedings of the Institution of Mechanical Engineers, Part G: Journal of Aerospace Engineering 0954410014544179, first published on July 29, 2014 doi:10.1177/0954410014544179
45. Suñol, A. and Vucinic D., (2014) "Numerical analysis and UAV application of the ACHEON vectorial thrust nozzle", 32nd AIAA Applied Aerodynamics Conference. June 2014. doi: 10.2514/6.2014-2046.
46. Das, S., Páscoa, J., Trancossi, M., and Dumas, A., "Computational Fluid Dynamic Study on a Novel Propulsive System: ACHEON and Its Integration with an Unmanned Aerial Vehicle (UAV)." J. Aerosp. Eng., 2016, doi:10.1061/(ASCE)AS.1943-5525.0000498, 04015015.
47. Zhuang N., Xiang J., Luo Z., and Ren Y., “Calculation of helicopter maneuverability in forward flight based on energy method”, Computer Modelling & New Technologies, 18(5), pp. 50-54, 2014.
48. McCormick, Jr., B. W., “Aerodynamic of V/STOL Flight”. Academic Press, pp. 154, 1967.
49. Bejan, A., “The evolution of airplanes”, J. Appl. Phys. 116, 044901, 2014; http://dx.doi.org/10.1063/1.4886855.
50. Bejan, A., “A bird? A plane? It’s all evolution”, Aerospace America, November, 2014.
51. Bejan A., and Lorente S., "Constructal theory of generation of configuration in nature and engineering", J. Appl. Phys., 100, 2006, doi:10.1063/1.2221896.
52. Bejan A., and Lorente S., "The constructal law of design and evolution in nature", Philosophical Transactions of the Royal Society B, 365: 1335-1347, 2010.
53. Bejan A., and Lorente S., "The Constructal law and the evolution of design in nature", Physics of Life Reviews, 8:209–240, 2011.
54. VV.AA., "Ansys Fluent 16.2", Ansys, 2015.
55. Gameiro Lopez, A. M., "EasyCFD 4.3.4" ADAI - Departament of Mechanical Engineering, University of Coimbra (2016)
56. ASME Editorial Board, "Journal of Heat Transfer Editorial Policy Statement on Numerical Accuracy," ASME Journal of Heat Transfer, Vol. 116, November 1994. pp. 797-798.
57. Coleman, H.W. and F. Stern, "Uncertainties and CFD Validation," ASME Journal of Fluids Engineering, Vol. 119, December 1997, pp. 795-803.
58. Roache, P.J., "Quantification of Uncertainty in Computational Fluid Dynamics," Annual Review of Fluid Mechanics, Vol. 29, pp. 123-160, 1997.

 

59. Jameson, A. and L. Martinelli, "Mesh Refinement and Modeling Errors in Flow Simulations,"AIAA Journal, Vol. 36, No. 5, pp. 676-686, 1998
60. Oberkampf, W.L. and T.G. Trucano, "Validation Methodology in Computational Fluid Dynamics" AIAA Paper 2000-2549, 2000.
61. VV.AA., Plettemberg Orbit Series Manual, Plettemberg Electromotoren, 2014 http://www.plettenberg-motoren.net/index.php/en/plettenberg-motors/plettenberg-brushless-motors/orbit/orbit-15-heli-expert
62. Technical datasheet - Product Deprom White, depronfoam.com - source data provided by Depron® international distributor, 2014, http://www.depronfoam.com/depron-foam/resource/Depron-White-Technical-Data-Sheet.pdf